Motor Control, 2004, 8, 312-338

Modeling Kinematics and Dynamics of Human Arm Movements

Marjan A. Admiraal, Martijn J.M.A.M. Kusters, and Stan C.A.M. Gielen

A central problem in motor control relates to the coordination of the arm's many degrees of freedom. This problem concerns the many arm postures (kinematics) that correspond to the same hand position in space and the movement trajectories between begin and end position (dynamics) that result in the same arm postures. The aim of this study was to compare the predictions for arm kinematics by various models on human motor control with experimental data and to study the relation between kinematics and dynamics. Goal-directed arm movements were measured in 3-D space toward far and near targets. The results demonstrate that arm postures for a particular target depend on previous arm postures, contradicting Donders's law. The minimum-work and minimum-torque-change models, on the other hand, predict a much larger effect of initial posture than observed. These data suggest that both kinematics and dynamics affect postures and that their relative contribution might depend on instruction and task complexity.

Key Words: posture, reaching, Donders's law

The human arm is a multiarticulate limb with many degrees of freedom, providing a large degree of flexibility. This flexibility also allows a particular simple motor task to be executed using various postures. In this context it is surprising that several studies have shown that the kinematics of arm postures are quite consistent and reproducible within and across participants (e.g., Soechting et al., 1995). In addition to postural flexibility at the endpoint of a movement, the arm's many degrees of freedom allow many different movement trajectories, bringing the hand from the initial position to a given end position. Nonetheless, the path of the index finger during a reaching movement has been reported to be consistent from trial to trial both within participants and across participants (Georgopoulos et al., 1981; Soechting & Lacquaniti, 1981).

The fact that movement kinematics and dynamical movement trajectories are consistent within and between participants has raised the question, to what extent are movement kinematics and movement dynamics related. One possibility might

The authors are with the Dept. of Biophysics, University of Nijmegen, the Netherlands.

be that movements are planned at a kinematic level (e.g., in joint coordinates or in extrinsic coordinates) and that once such a plan exists, the forces to produce the desired movement trajectory are generated. This class of models is usually referred to as "posture based." One particular model of this type is Donders's law, originally proposed for eye movements. It states that torsion of the eye is uniquely determined for each gaze direction (Donders, 1848; Tweed & Vilis, 1987). Later studies have reported that Donders's law is also obeyed for head and arm movements (Hore et al., 1992; Miller et al., 1992; Straumann et al., 1991). More detailed analyses, however (Gielen et al., 1997; Soechting et al., 1995), revealed small but systematic deviations from the unique torsion for pointing directions inconsistent with Donders's law. Another type of posture-based prediction follows from the equilibrium-trajectory hypothesis (Flash, 1987; Hogan, 1985), which states that the trajectories are achieved by gradually shifting the hand equilibrium positions between the begin and endpoint of movements.

Another possibility might be that movement trajectories are the result of some optimization process or might be the result of some dynamical constraints and that kinematics are a result of movement dynamics. An example from this class of models is the minimum-work model (Soechting et al., 1995). Soechting and colleagues suggested that the deviations of Donders's law could be explained by assuming that movements are made based on the criterion of minimization of work. This implies that final posture of a movement is the result of minimizing the amount of work that must be done to transport the arm from the starting posture toward a target. The minimum-work hypothesis is an alternative for sequential planning of kinematics and dynamics. According to this hypothesis, the dynamics and kinematics follow tightly connected from the optimization criterion, given the movement time and the initial and final position of the movement. The same is true for other optimization models that have been proposed to explain the reproducible nature of movement trajectories, such as the minimum-torque-change model (Uno et al., 1989), the minimum-commanded-torque-change model (Nakano et al., 1999), the minimum-variance model (Harris & Wolpert, 1998), and the stochastic optimal-control model proposed by Todorov and Jordan (2002).

Obviously, these models cannot all be correct. In this context, it is remarkable to note that a quantitative comparison between the performances of these models for movements in 3-D space has not yet appeared. Such a comparison would be important for several reasons. First, it could discriminate between viable models and models that must be rejected. Second, a quantitative comparison could reveal whether a single model can provide a good fit to the data or whether the central nervous system might use multiple criteria, with each criterion suitable for one or a small set of contexts (see, e.g., Haruno et al., 1999, 2001). In that case, it might be that a model gives a good performance for a particular set of movements or movement instructions but fails for another. Given the different optimization criteria of the various models (e.g., minimum-work, minimum-torque-change), it might well be that the performance of the models depends on the context and instruction to the participant, as was proposed by Todorov and Jordan (2002).

The aim of this study was to investigate arm movements to distant targets with the fully extended arm ("pointing movements") and movements between various

targets in 3-D space at various distances relative to the participant, requiring flexion or extension of the elbow ("reaching movements"). Participants were instructed to make arm movements toward randomly presented targets. To investigate whether the central nervous system might use multiple criteria, with each criterion suitable for one or a small set of contexts (see, e.g., Haruno et al., 1999, 2001), participants were tested at three different movement velocities: (a) without any instruction regarding velocity, where movement velocity was freely chosen by the participant, and with the instructions to (b) "move as accurately as possible" or to (c) "move fast." The aim was not to generate a new unique set of data, because many studies have collected similar data. Rather, these data were collected to serve as a reference to test the predictions by the minimum-work model and the minimum-torque-change model. As will be explained later, the predictions of arm postures by the minimum-commanded-torque-change model and the minimum-variance model for the fully extended arm (including torsion along the long axis of the arm) are similar to the predictions by the minimum-work model for many initial and final targets. The predictions by these movements were compared with the null hypothesis of a unique posture for each target position (Donders's law). We have not tested the equilibrium-point (EP) hypothesis, because it has many versions: It can be formulated at the single-muscle level, at a single-joint level, and at a single-effector level. Therefore, the EP hypothesis, as it now stands, cannot make unambiguous general predictions with respect to arm postures.

Methods

Fifteen individuals age 21–49 years ■participated in the experiments. None had any known sensory, perceptual, or motor disorders. All gave informed consent to participate, and none were familiar with the purpose of the study. All participants were right-handed, and all movements were made with the right arm. Two experiments were performed, and participants took part in either the pointing experiment (6 participants) or the reaching experiment (9 participants). The experimental protocols were approved by the medical-ethical committee of the University of Nijmegen, and all participants gave informed consent before the experiment.

Experimental Setup

Visual stimuli generated by a personal computer were projected by an LCD projector (Philips Proscreen 4750) on a translucent screen. The visual scene projected on the screen covered an area of 120 × 96 cm, corresponding to a maximum visual range for the participant of 62 × 51° in the pointing experiment and 74 × 62° in the reaching experiment. In the pointing experiment, the computer generated a video image of a checkerboard pattern with 8 × 8 alternating black and yellow rectangles (15 × 12 cm each) on the projection screen. The pointing targets (yellow spheres with a diameter of 1.5 cm) were projected on top of this background. In the reaching experiment, the computer generated a video image of a virtual 3-D scene on a plane parallel to the projection screen. The video image consisted of two images of the scene, one in green, representing the projection of the 3-D scene as viewed by the left eye, and one in red, representing the projection of the 3-D scene as viewed by

the right eye. Participants wore a pair of goggles with a red filter (Kodak Wratten nr. 25) for the right eye and a green filter (Kodak Wratten nr. 58) for the left eye, providing stereo vision. Targets for the reaching movements were small yellow spheres (diameter 1.5 cm) that appeared in front of a checkerboard background consisting of 8 × 8 alternating black and yellow rectangles (15 × 12 cm each). The images for the left and right eyes were generated in the proper perspective relative to the observer, such that the checkerboard background appeared at a distance of about 10 cm in front of the projection screen as seen by the observer.

The participants sat on a chair with a straight and high back support. The position and height of the chair could be adjusted such that their right shoulder was in front of the center of the visual scene. In the pointing task, the participant's body was rotated 45° relative to the projection screen, whereas in the reaching task the participant was positioned in front of the projection screen (see Figure 1). Participants were secured to the chair by seat belts that allowed all rotations in the shoulder but kept the trunk and shoulder in a fixed position in space throughout the experiment. This was verified by measuring the position of an infrared-light-emitting diode (IRED) on the shoulder with the Optotrak® system (NDI, Waterloo, ON).

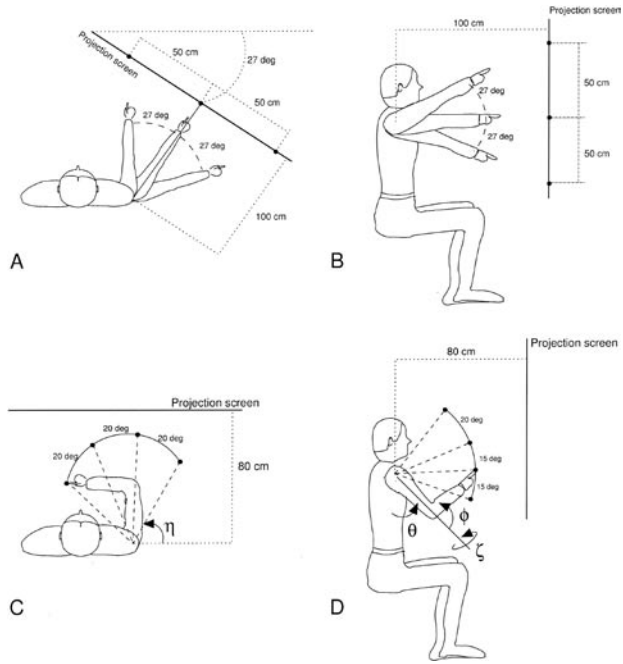

Figure 1 — Top and side views of the participant for the pointing and reaching experiment. Panels A and B represent top and side views, respectively, of the experimental setup in the pointing experiment. Panels C and D represent the top and side views of the experimental setup in the reaching experiment. The definition of rotation angles (η, θ, ζ, and φ) used to define the arm's orientation in the reaching experiment is indicated by arrows in Panels C and D.

The position and orientation of the upper arm were measured with an Optotrak system capable of measuring the positions of the IREDs with a resolution better than 0.2 mm in a range of 1.5 m^3. The Optotrak system was mounted on the ceiling above the participant at a distance of approximately 2.5 m behind the participant, tilted downward at an angle of 30° relative to the ceiling. Movements were sampled at a rate of 100 Hz.

A cross with IREDs on each of the four tips was attached to the upper arm just proximal to the elbow joint and at the forearm just proximal to the wrist joint. The lengths of the arms of the crosses were 6 and 12 cm for the crosses on the forearm and upper arm, respectively. Additional (single) IREDs were attached to the shoulder (acromion), the elbow (epicondyle lateralis), and the tip of the index finger. Participants were instructed to keep the index finger in full extension such that the forearm, hand, and index finger were all aligned.

Experimental Paradigms

Participants were tested in two experiments. The first, the pointing task, focused on pointing movements with the fully extended arm to targets displayed on the projection screen at a distance of 100 cm (range 54° in both azimuth and elevation). In the second experiment, the reaching task, targets appeared in various directions and at various distances relative to the shoulder (range 60° in azimuth and 50° in elevation), requiring flexion of the arm (see Figure 1). By definition, a vertically downward orientation of the upper arm corresponds to an elevation angle (θ) of 0°. The azimuth angle (η) is positive when the upper arm is directed leftward, negative when it is oriented to the right, and zero for the straight-ahead direction. When the elbow is fully extended, the flexion angle (ϕ) is defined to be zero; flexing the elbow corresponds to positive flexion. Torsion (ζ) is defined as the rotation around the humeral axis of the upper arm. With 0° of torsion, the upper arm and forearm lie in a vertical plane for all flexion angles.

In both experiments, we tested arm movements in a task that sets all but one available degrees of freedom. In the pointing task, this remaining degree of freedom corresponds to the torsion of the arm, whereas in the reaching task, it lies in the combination of angles θ, η, and ζ. Setting one of these three angles defines the other two. Hence, the outcome of the analysis does not depend on which angle is evaluated. For consistency, we chose to evaluate the amount of torsion of the upper arm (ζ) both in the pointing experiment and in the reaching experiment.

Pointing Task

In the first experiment, participants sat with their right shoulder at a distance of 100 cm in front of the projection screen. Five bright-yellow, spherical targets with a diameter of 1.5 cm were displayed on top of the checkerboard pattern on the projection screen. Four target positions were located at each corner of a 100-cm by 100-cm square, numbered clockwise I to IV, starting with the upper left target. The fifth target (V) was located in the middle of the square, directly in front of the right shoulder (see Figure 2A). When pointing to these four targets, the azimuth angles in the shoulder ranged from –27 to +27°, and elevation angles ranged from –27 to +27°. Participants had to point to the targets with the fully extended arm.

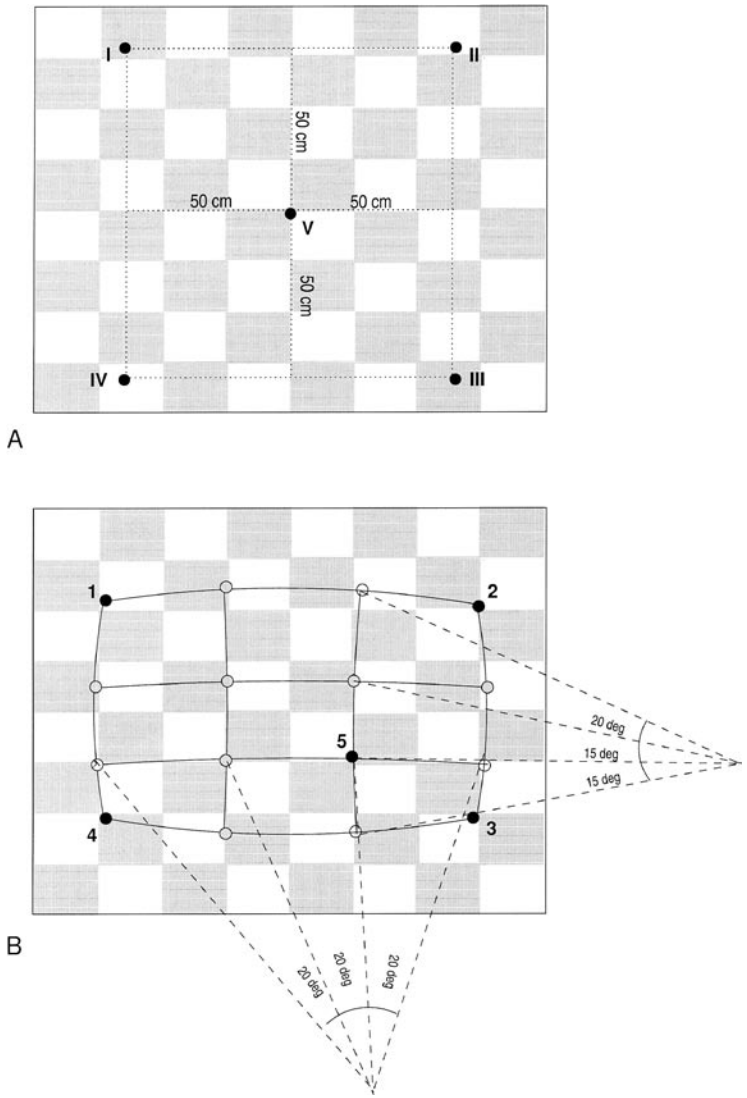

Figure 2 — Targets for the (A) pointing and (B) reaching experiments. In Panel A, the filled symbols represent the targets, projected on the screen, toward which participants were asked to point with the extended arm. The filled symbols in Panel B represent the initial and final targets used for the analysis. The open symbols correspond to targets for movements that were not included in the analysis. Targets V and 5 corresponded to a position straight in front of the right shoulder (see Figure 1). In Panel B, dashed lines indicate the azimuth (bottom) and elevation (right) position of the targets relative to the right shoulder.

At the start of each trial, participants were instructed to point at Target V for about 1 s and then to Target I. From there, the pointing movement moved either in a clockwise direction (order I-II-III-IV-I) for about eight cycles or in a counterclockwise direction (order I-IV-III-II-I) for eight cycles. Participants were instructed to make arm movements from one target to the next, while stopping at each target for a short period after each movement.

Each movement direction was tested with three instructions. In the first set of trials, participants were instructed to move from one target to the next with a smooth, self-paced movement (self-paced). In the second type of trial, participants were instructed to move fast from one target to the next but told to stop their movement at each target before moving to the next (fast). In the third type of trial, participants were instructed to move to each target with a single, smooth movement but to do so as accurately as possible (accurate). Each type of instruction was repeated two times (fast and accurate) or four times (self-paced) for both movement directions.

At the end of this series of experiments, participants were asked to point at random in various directions with the fully extended arm. These postures were used to estimate the dependence of torsion of the upper arm on azimuth and elevation for various directions of azimuth and elevation. According to Donders's law, torsion should be uniquely determined for each direction of azimuth and elevation (see Models).

Reaching Task

For the second experiment, the participant's shoulder was placed at a distance of 80 cm from the screen (see Figures 1C and 1D). In this experiment, we tested postures of the arm when participants reached toward a virtual target within reaching distance in 3-D space. Participants were asked to position the tip of the index finger at the virtual target position until it disappeared and a new target appeared. They were instructed to maintain their current posture after each movement until they accurately localized the new target before making a single aiming movement toward it. When the new target was not found or not perceived accurately because it appeared partly obstructed by the participant's arm, participants were instructed not to make a movement but to wait for the next target to appear.

For each participant, we adjusted the target positions so that the targets appeared at equal distances relative to the shoulder corresponding to elbow flexion near 90° when the participants reached the target correctly. Targets appeared at 1 of 16 locations on a grid, such that movements to neighboring targets required changes of 20° in azimuth and 20 or 15° in elevation relative to the shoulder (see bottom panels in Figure 1 and Figure 2B). The target remained at its location for 2 s. Targets appeared in a pseudorandom order for all participants. In the analysis we selected only movements starting or ending at one of the four targets at the corners of the grid (Targets 1, 2, 3, and 4) and at a location straight ahead of the right shoulder (Target 5). Using these five positions as begin and end targets for aiming movements yields 20 possible combinations. All participants made at least five movements for each of these 20 target pairs.

Because we examined whether postures of the arm were dependent on postures for previous targets, we tried to arrange the same initial posture at the beginning of

each series of movements. According to Soechting et al. (1995), postures should be most reproducible when the right arm is pointing to a target at the lower left side. Therefore, each pair of targets from the 20 combinations was preceded by Target 4 (the lower left target, at –40° azimuth and –15° elevation).

To prevent fatigue, participants were tested in 10 blocks with 15 movements each. Participants could pause between blocks as long as they needed.

Models for Movement Planning

Donders's Law

Donders's law assumes that the central nervous system uses a unique orientation of the upper arm for each position of the hand. The orientation of the upper arm during pointing is expressed in terms of a rotation axis and rotation angle that rotates the upper arm from a reference position to the current position. This rotation vector is defined by

$$\vec{r} = \tan\left(\frac{\alpha}{2}\right) \vec{n} \tag{1}$$

where $\vec{n}$ represents the unit vector of the rotation axis in 3-D and α is the angle of rotation along that axis (see, e.g., Haustein, 1989; Straumann et al., 1991). When the right position (the so-called primary position; see Haustein, 1989) is taken as a reference position, the three orthogonal components of rotation vector $\vec{r}$ (r_u, r_v, and r_w) represent the torsional, elevation, and azimuth components, respectively. The relation between torsion angle (ζ) and the torsional component r_u follows from the definition in Eq. 1, where $\vec{r}$ equals r_u when $\vec{n}$ is along the humeral axis of the upper arm, and $\alpha = \zeta$.

Donders's law assumes that torsion is fully specified by azimuth and elevation of the upper arm while pointing. A polynomial fit was used to find the relation of the torsional component r_u as a function of r_v and r_w (see Gielen et al., 1997).

The Minimum-Work Model

The model for calculating minimum work was first presented by Soechting and colleagues (1995). In agreement with their findings, we use a coordinate system to define target location and arm posture: The *x* axis is in the lateral direction passing through the shoulders, and the *y* axis is directed forward relative to the right shoulder, from which the *z* axis points upward. Because the participant's shoulder is strapped tightly to the chair, this *x*-*y*-*z* coordinate system is fixed in space. Pronation and supination of the forearm were not evaluated because they do not affect the position of the index finger in space and because the wrist was kept straight throughout the experiments. Next, four joint angles are required to uniquely define the posture of the arm in this coordinate system—three angles that describe rotations at the shoulder joint and one that describes elbow flexion or extension (see Figure 1).

The amount of work, *W*, that is necessary to move the arm from one point to another is given by

$$W = \int \vec{T} \cdot d\vec{\Theta} \tag{2}$$

where $\vec{T}$ is the vector with torques in the shoulder and elbow and $\vec{\Theta}$ is the vector with joint angles in the shoulder and elbow. Ignoring gravitational forces, the amount of work done at time *t* is defined as the difference between kinetic energies at the position at time *t* and starting position. Because the arm starts from rest, its kinetic energy at the starting position is zero. Therefore, work at some time *t* can be written as

$$W = \int \vec{T} \cdot \vec{\Omega} dt = \sum_{i=1,2} \left[\frac{1}{2} m_i \vec{v}_i^{\,T} \cdot \vec{v}_i + \frac{1}{2} \vec{\Omega}_i^{\,T} \cdot I_i \cdot \vec{\Omega}_i \right] \tag{3}$$

where parameter i = 1, 2 refers to the two segments, forearm and upper arm, $\vec{\Omega}_i = d\vec{\Theta}_i / dt$, and m_i is the total mass of either the upper arm or the forearm, $\vec{v}_i$ is the speed of the arm's center of mass, and I_i is the inertia tensor of the arm.

When the rotations of the upper arm are described in a coordinate system [X\prime\, Y\prime\, Z\prime\] centered in the right shoulder instead of the Cartesian coordinates [*X, Y, Z*] (see Soechting et al., 1995), the three separate components of the angular-velocity vector of the upper arm read

$$\begin{aligned} \Omega_{X'} &= \dot{\eta} \sin\varsigma \sin\theta + \dot{\theta} \cos\varsigma \\ \Omega_{Y'} &= \dot{\eta} \cos\varsigma \sin\theta - \dot{\theta} \sin\varsigma \\ \Omega_{Z'} &= \dot{\eta} \cos\theta + \dot{\varsigma} \end{aligned} \tag{4}$$

Assuming that the upper arm and forearm can be considered solid cylinders, their moments of inertia, computed about the center of mass, are the same for rotations in azimuth and elevation (I_{u1}, I_{f1}). Rotations around the humeral axis of the upper arm meet a much smaller moment of inertia (I_{u2}).

The velocity of the arm's center of mass can be computed from the vector cross-product between the angular-velocity vector $\vec{\Omega}$ and the vector $\vec{r}$ connecting the shoulder to the arm's center of mass: $\vec{v} = \vec{\Omega} \times \vec{r}$.

After some algebra, one obtains for the work, *W*,

$$\begin{aligned} W = \frac{1}{2} \Big[& I_1 \left(\Omega_X^{\,2} + \Omega_Y^{\,2} \right) + I_2 \Omega_Z^{\,2} \\ & + I_3 \left(\left(\Omega_x + \dot{\phi} \right)^2 + \left(\Omega_Y \cos\phi + \Omega_Z \sin\phi \right)^2 \right) + I_4 \left(\Omega_Y \sin\phi - \Omega_Z \cos\phi \right)^2 \\ & + 2A \left(\left(\Omega_X^2 + \Omega_Y^2 \right) \cos\phi + \Omega_Z \Omega_Y \sin\phi + \dot{\phi} \Omega_X \cos\phi \right) \Big] \end{aligned} \tag{5}$$

With the use of Eq. 6, this can also be written as

$$\begin{aligned} W = \frac{1}{2} \Big[& I_1 \left(\dot{\eta}^2 \sin^2\theta + \dot{\theta}^2 \right) + I_2 \left(\dot{\eta} \cos\theta + \dot{\varsigma} \right)^2 \\ & + I_3 \left(\Omega_X^2 + \Omega_Y^2 \cos^2\phi + \Omega_Z^2 \sin^2\phi + \dot{\phi}^2 + 2\dot{\phi}\Omega_X + 2\Omega_X \Omega_Y \cos\phi \sin\phi \right) \\ & + I_4 \left(\Omega_Y^2 \sin^2\phi + \Omega_Z^2 \cos^2\phi - 2\Omega_Z \Omega_Y \cos\phi \sin\phi \right) \\ & + 2A \left(\left(\Omega_X^2 + \Omega_Y^2 \right) \cos\phi + \Omega_Z \Omega_Y \sin\phi + \dot{\phi}\Omega_X \cos\phi \right) \Big] \end{aligned} \tag{5a}$$

which is similar—but not equal—to the equation for the total amount of work presented by Soechting et al. (1995). Equation 5a includes an extra term in the total work that corresponds to

$$\frac{A}{2}\left[\left(\Omega_X^2 + \Omega_Y^2\right)\cos\phi + \Omega_Z\Omega_Y \sin\phi + 2\dot{\phi}\Omega_X \cos\phi\right] \tag{6}$$

Because we started from the same equations for the angular velocities that Soechting and colleagues used, we expect this discrepancy to be a typographical error in Soechting's equation. The appendix shows a more detailed derivation of our equation.

When we ignore the effect of gravity, the total work done during the movement is zero because the final velocity is zero. The positive work done to accelerate the arm is canceled by the negative work required to decelerate the arm at the end of the movement. Similar to Soechting et al., we assume that movement velocities are bell shaped and that joint velocities in elbow and shoulder reach a peak value at the same time. The work will have a peak positive value at the time of peak velocity. Because of the bell-shaped velocity profiles, the peak value of kinetic energy is reached halfway through the movement. The work related to this peak value of kinetic energy is used as cost for the minimization of work.

The Minimum-Torque-Change Model

All simulations of the minimum-torque-change model in the literature have been done for movements in a 2-D plane. In this article we have used the minimum-torque-change model of Uno et al. (1989) to describe arm movements in 3-D space. The cost function to be minimized (C_T) is the sum of squares of the rates of change in torque integrated over the duration of the entire movement (t_m):

$$C_T = \frac{1}{2}\int_{t=0}^{t_m}\sum_{i=1}^{N}\left(\frac{dT_i}{dt}\right)^2 dt \tag{7}$$

where T_i is the torque generated by the ith actuator (joint) out of N joints evaluated. To calculate the torque, we used the Lagrange formalism

$$L(q, \dot{q}, t) = K(q, \dot{q}, t) - V(q) \tag{8}$$

with $\vec{K}$ the kinetic energy and $\vec{V}$ the potential energy. As in previous studies, we ignored gravity and set the potential energy $\vec{V}$ to zero. The torques follow from the Lagrange equation of motion:

$$\vec{T} = \frac{d}{dt}\left(\frac{\partial L}{\partial \dot{\vec{q}}}\right) - \frac{\partial L}{\partial \vec{q}} \tag{9}$$

The equation for the torques that result from the Eq. 9 is rather complex and will not be shown here.

Like Uno et al. (1989) we introduce a set of nonlinear differential equations to find the trajectory corresponding to minimum torque change,

$$\frac{d\vec{\Xi}}{dt} = \vec{f}\left(\vec{\Xi}, \vec{u}\right)$$
$$\frac{d\vec{\psi}}{dt} = -\left(\frac{\partial \vec{f}}{\partial \vec{\Xi}}\right)^T \vec{\psi} \qquad (10)$$
$$\vec{u} = \begin{bmatrix} dT_\theta/dt \\ dT_\eta/dt \\ dT_\xi/dt \\ dT_\phi/dt \end{bmatrix}$$

where $\vec{\Xi}$ is a 3-*N*- (in this case 12-) -dimensional vector with the four joint angles (θ, η, ς, and ϕ) as the first four components (same definitions as for the minimum-work model, see Figure 1), the first time derivatives of the joint angles as the next four components ($\dot{\theta}$, $\dot{\eta}$, $\dot{\varsigma}$, and $\dot{\phi}$), and the torques in these joints as the last four components (T_θ, T_η, T_ς, and T_ϕ). The vector $\vec{\psi}$ represents a Lagrange-multiplier vector with 3-*N* components, of which the last *N* components are equal to the vector $\vec{u}$.

Eq. 10 represents an autonomous nonlinear differential equation with respect to $\vec{\Xi}$ and $\vec{u}$ (Uno et al., 1989). In this way, our optimization problem results in a boundary-value problem, which can be solved in an iterative way, based on a Newton-like method.

The initial value of $\vec{\Xi}$ at time zero is specified (i.e., $\vec{\Xi}(t_0) = \vec{\Xi}_0$). The initial value of $\vec{\psi}$ is unknown, however, because the begin values for the torque change are unknown. Therefore, when we assume a particular initial value of $\vec{\psi}(t_0)$ and solve the initial-value problem for the differential Eq. 10, the final value $\vec{\Xi}(t_f)$ will not reach the target value $\vec{\Xi}_f$. Therefore, we define a residual error at t_f as

$$\vec{E} = \vec{\Xi}_f - \vec{\Xi}(t_f) \qquad (11)$$

This error $\vec{E}$ is a function of the initial value $\vec{\psi}(t_0)$. The optimal trajectory, which obeys the constraints of minimum torque change and minimizes the error function $\vec{E}(\vec{\psi})$, is found in the same way as described by Uno et al. (1989), based on a steepest-gradient method of $\vec{E}(\vec{\psi}(t))$ with respect to the initial vector $\vec{\psi}(t_0)$ using a Newton-like iteration procedure.

Predictions for Movement Trajectories and Orientations of the Upper Arm

When the fully extended arm is modeled as a solid cylinder, the inertia is the same for movements in elevation and azimuth. If movements of such a cylinder are constrained by an efficiency criterion such as predicted by the minimum-work hypothesis (Soechting et al., 1995) or by minimum-torque change (Uno et al., 1989), rotations of the fully extended arm in the shoulder should be single-axis rotations taking the shortest path from initial to final position. This implies that the direction of the angular-velocity vector $\vec{\Omega}$ is in the direction of $\vec{r}_1 \times \vec{r}_2$, where $\vec{r}_1$

and $\vec{r}_2$ represent the positions of the index finger relative to the shoulder for initial and final target positions, respectively, and where $\times$ represents the vector-product operator. Such shortest-path rotations correspond to movements along the geodete of a sphere in workspace.

The arguments noted previously explain why the minimization models predict movements over the geodete of a sphere for pointing movements with the fully extended arm. It is well known, however, that movements along a closed path by a concatenation of subsequent movements following the geodetes that connect the initial and final positions of the via points give rise to an accumulation of torsion (see Gielen, 1993; Tweed & Vilis, 1987). This implies that the orientation of the upper arm should depend on the number of previous clockwise or counterclockwise cycles. Donders's law, however, predicts that orientation of the upper arm for a particular pointing direction is constant, irrespective of the number of previous clockwise or counterclockwise cycles. In the pointing experiment we tested these predictions by asking participants to make clockwise or counterclockwise movements between the corners of a square (Targets I, II, III, and IV in Figure 2A).

The predicted torsion follows from straightforward application of differential geometry, which predicts that the accumulation of torsion after a cycle is equal to the integral of the Gaussian curvature over the area bounded by the trajectory of the cycle (see Stoker, 1989)■:

$$\Delta\zeta = \oint \frac{1}{R^2}\, dA \tag{12}$$

For the clockwise and counterclockwise movements in the pointing experiment, the Gaussian curvature corresponds to R^{-2}, where R is the distance between the index finger and the shoulder. The accumulation of torsion would then total about 49° per cycle. An accumulation of torsion contradicts Donders's law, which predicts a unique torsion for each target.

Results

Pointing with the Fully Extended Arm

In the first experiment, participants were asked to point with the arm extended to targets presented at different elevation and azimuth positions at a distance of 100 cm from the participant's shoulder that was fixed in space (see Methods). Figure 3 shows the measured trajectories (dotted lines) of the index finger for participant HP for repeated movements between the corners of a square in a clockwise direction (Panel A) and in a counterclockwise direction (Panel B). For pointing with the fully extended arm, the minimum-torque and minimum-work models give the same predictions for the trajectory of the index finger, indicated by solid lines. These predicted trajectories correspond to rotations in the shoulder about the shortest angle from begin to end target (see Methods). They lead to curved trajectories along the geodete on the surface of the sphere with the center at the shoulder and a radius equal to the length of the arm. The measured and predicted trajectories are shown in a 2-D projection on the frontal plane (see Figure 1).

In general, the measured and predicted trajectories are quite similar, except for the movements between Targets I and II in a clockwise direction (Figure 3A), where the measured trajectories deviated systematically from the predicted trajectories. For other movements—for example, between Targets II and III and between Targets III and IV in the clockwise direction (Figure 3A) and between Targets II and I in the opposite direction (Figure 3B)—the measured trajectories deviated slightly from the predicted trajectories in some trials.

The apparent correspondence between the measured and predicted trajectories of the index finger in space does not prove that the predictions of the minimization models are correct, because the data in Figure 3 do not provide information about torsion along the humeral axis of the arm. A consequence of the predictions by the minimization models is that rotations in the shoulder are rotations along the shortest path, resulting in an accumulation of torsion in the upper arm for movements along a closed trajectory. The predicted accumulation in torsion is either positive (increase in torsion) for movements in the clockwise direction (I to II, II to III, III to IV, and IV to I) or negative (decrease in torsion) for the counterclockwise movements (I to IV, IV to III, III to II, and II to I). Thus, with each full cycle the amount of torsion at a target position will be larger or smaller than at the previous trespassing. This prediction contradicts Donders's law, which predicts a unique amount of torsion for each target position.

Figure 4 shows the measured change in torsion of the upper arm for the first six cycles for 6 participants. Because changes in torsion are not significantly different for various targets, each data point shows the change of torsion of the upper arm

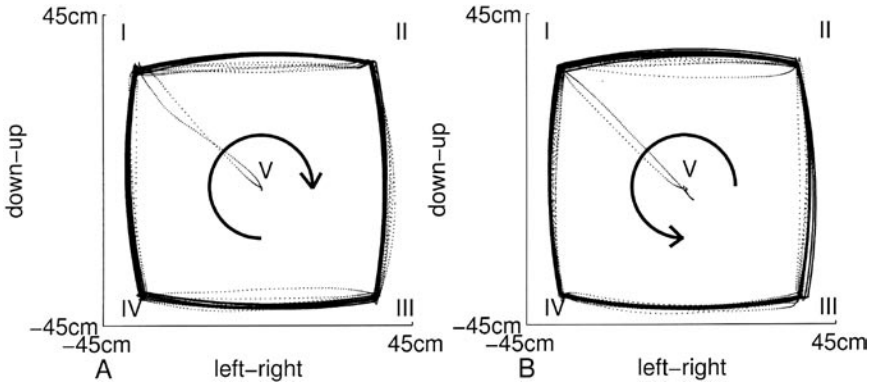

Figure 3 — Projection on the frontal plane of the measured and predicted trajectories of the index finger between the corners of a square in a clockwise direction (Panel A) and in a counterclockwise direction (Panel B). Data are shown for 1 participant (Participant HP). Solid lines represent the trajectories corresponding to the predictions by the minimum-work and minimum-torque-change models (the shortest path along the surface of a sphere, so-called geodetes). Dotted lines represent the measured trajectories of the index finger. Positions I, II, III, and IV indicate the endpoints of the movements on the corners of a square. Position V indicates the initial and final pointing direction.

averaged over all four targets for subsequent cycles relative to the torsion at the first passage through the target. The change in torsion is displayed separately for the clockwise cycles (upper panels) and counterclockwise cycles (lower panels) for the self-paced, accurate, and fast-movement conditions (left, middle, and right panels, respectively).

Panels A and D show the measured torsion of the upper arm for self-paced clockwise and counterclockwise cyclic movements, respectively, for each cycle averaged over all targets. For the clockwise cycles (top panels), the amount of torsion is significantly larger after the first cycle than at the beginning of the first cycle for all participants. After the second cycle, torsion remains more or less constant; torsion in the third cycle is not significantly larger than in the second cycle. The standard deviation of torsion in the data is very similar for all participants and for all cycles (range 1–7°, $M = 3 \pm 1.5°$).

The data in Figures 4A and 4B show that torsion typically increases for the first two cycles until it has accumulated to about 5–15°. This result does not correspond to

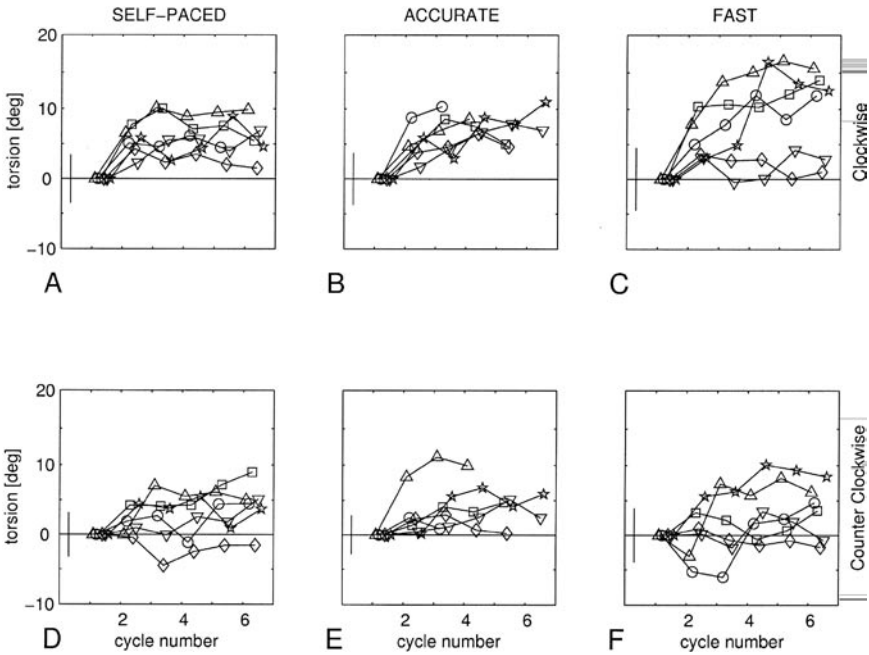

Figure 4 — Changes in torsion, averaged over all four targets, for cyclic pointing movements relative to torsion at the first passage of the target. Upper (lower) panels show changes in torsion for clockwise (counterclockwise) cycles for the self-paced, accurate, and fast conditions (left, middle, and right panels, respectively). The data of the 6 participants are indicated by different symbols. For different participants and cycle numbers, the *SD* is very similar (range 1–7°; $M = 3 \pm 1.5°$). Therefore, the mean *SD* is shown in each panel by error bars at the beginning of each axis, indicating the average *SD* for data in all cycles for all participants displayed in the panel.

the predictions by the minimization models. As explained in the Methods section, the minimum-torque-change and minimum-work models predict an accumulation of torsion for movements along a closed path that would correspond to an accumulation of torsion after each cycle by 49° for this experiment. Evidently, this is not case at all.

Previous studies have shown that instruction to the participant affects torsion of the upper arm (see, e.g., Medendorp et al., 2000). To investigate whether instruction to the participant might affect the accumulation of torsion in our study we also tested participants with the instruction to move accurately or fast. The results are qualitatively similar to the self-paced results in clockwise and counterclockwise cycles. For all conditions except the fast counterclockwise condition, the amount of torsion for all participants was significantly larger in the second cycle than in the first ($2.8 < t < 5.5$, $p < .05$) but does not increase significantly after the second cycle.

For the self-paced and accurate movements, the increase in torsion seems to be very similar between participants (most obviously in the clockwise cycles), whereas in

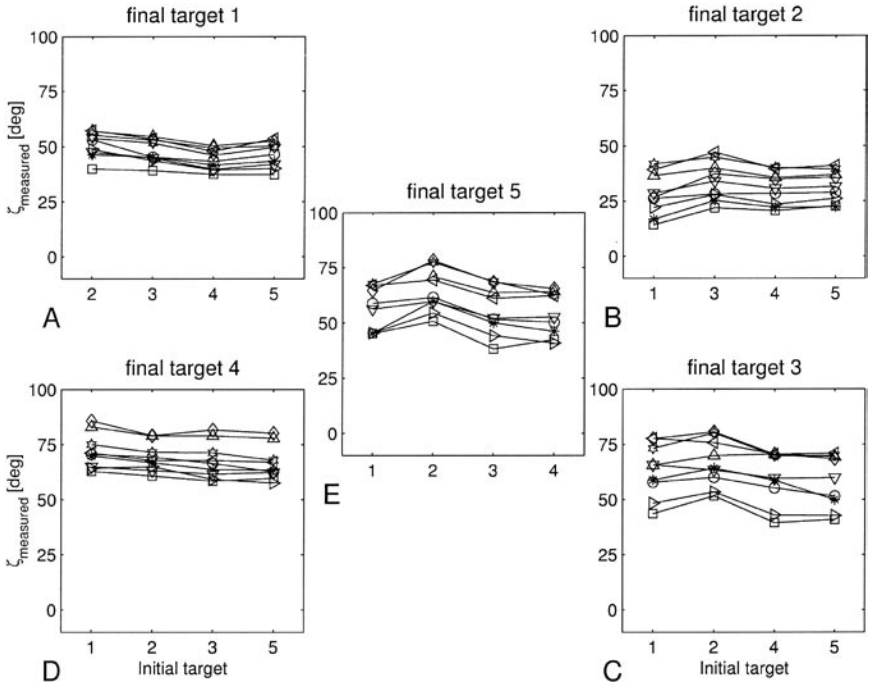

Figure 5 — Humeral axis-rotation angle as a function of initial position for postures of the upper arm at the end of movements toward Targets 1–5. Each panel shows the amount of torsion while reaching for one of the five final targets as a function of the initial position of the movement. Different symbols refer to data from different participants. Torsion of 0° corresponds to an orientation of the upper arm such that when elevation is 90°, the upper arm and forearm lie in a vertical plane, irrespective of elbow flexion.

the fast movements the increase in torsion is less consistent between participants. This effect of instruction was not significant, however (ANOVA, $p > .1$).

Remarkably, changes in torsion are qualitatively the same in the clockwise and counterclockwise directions, such that both tend to increase in the second cycle. This is surprising because the minimum-work and minimum-torque-change models predict accumulation of torsion in the negative direction for counterclockwise movements.

Torsion of the Upper Arm During Reaching Movements

Figure 5 shows the amount of torsion of the upper arm (angle ζ) while reaching for Targets 1–5 for movements starting from the other target positions. The results for each final position are displayed in separate panels arranged similarly to the target configuration (see Figure 2). Different symbols refer to data from different participants. In agreement with results of previous studies (Gielen et al., 1997; Soechting et al., 1995), Figure 5 clearly shows that the amount of torsion at the end of a movement depends on the initial position and that these effects are very consistent across participants. For each of the five possible endpoints, the deviation

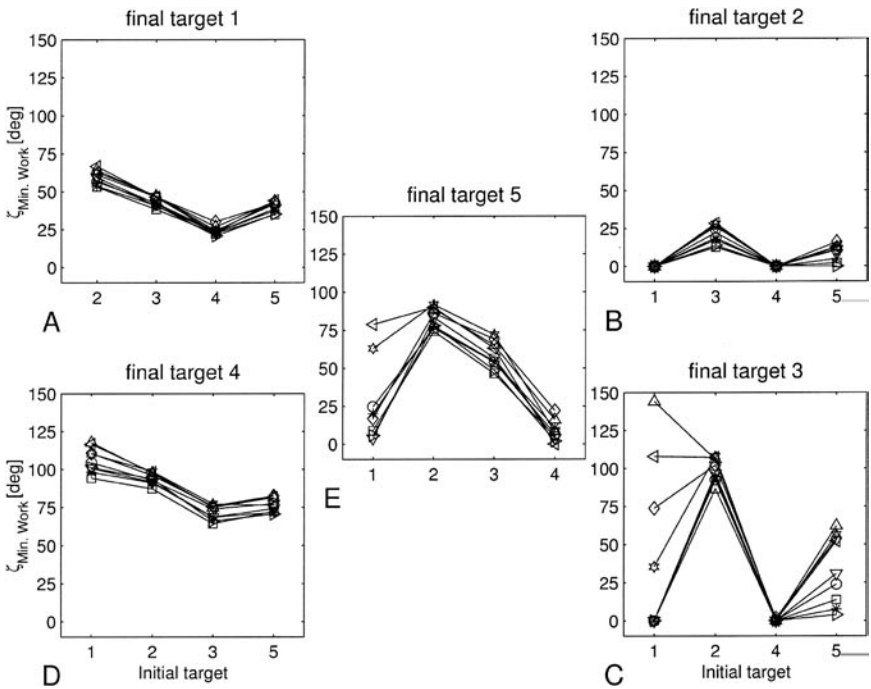

Figure 6 — Prediction of the humeral axis-rotation angle (ς) by the minimum-work model for movements to the five targets starting from different initial positions. For each participant, the mean posture at each begin position was used to predict the torsion at the end of the movement. Different symbols refer to predictions for different participants.

from the average torsion at the end position depends significantly on the initial position: ANOVA $F(3, 32) = 58.9$, 20.2, 22.5, 30.6, and 43.0 for Endpoints 1–5, respectively; $p < .001$ for all endpoints.

Torsion of the upper arm was also simulated according to the minimum-work model. For each reaching movement, the input to the model was the measured posture at the initial position and the final target position in space. Figure 6 shows the predicted torsion angle ζ for five final targets as a function of the initial target at the beginning of the movement. The large variation in predicted torsion for movements from Target 1 to final Targets 5 and 3 (middle panel and lower right panel, respectively) between participants results from variations in participants' initial posture at Target 1. The dependence of predicted torsion of the upper arm on initial posture of the arm is qualitatively similar to that shown in Figure 5. Qualitatively, however, the data are very different. The range of variation in torsion of the upper arm resulting from different initial postures is typically about 10° or less for each participant in the real data, whereas it varies from 20° (for final Target 2, in Figure 6B) to 100° (for final Target 3, in Figure 6E) for the minimum-work predictions.

To obtain a good overall comparison between the predictions by the minimum-work model and the measured data, we plotted the measured torsion of the upper arm against simulated torsion (see Figure 7). For each participant we plotted 20 data points corresponding to the averages of the repeated trials between the 20 possible pairs of initial and final targets. Different symbols in Figure 7 correspond to the different endpoints of the movements.

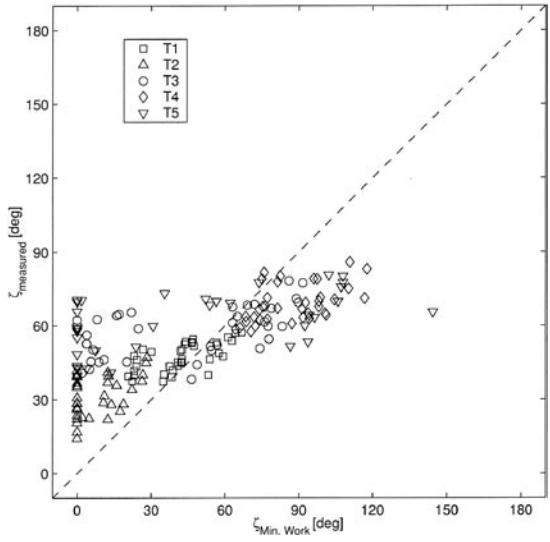

Figure 7 — Measured torsion of the upper arm (vertical axis) versus the predicted torsion according to the minimum-work model (horizontal axis). Different symbols refer to torsion at different final targets (see inset). For each participant, all end postures for a given pair of initial and final targets are averaged. Data in the figure correspond to the averages for each of the participants individually.

If predicted and measured torsion were the same, the data would lie on the line of unity. This is obviously not the case. Figure 7 clearly shows that the measured and predicted data are correlated ($R = .75$, $p < .01$). The slope of a linear regression is about .3, which is significantly different from unity. The figure shows that for a large part of the data, the minimum-work model predicts a final torsion of 0°. This is a consequence of the limits we chose for the minimization models, such that the predicted torsion would not exceed the (physical) range of torsion in the shoulder between 0 and 180°.

The predicted torsion of the upper arm by the minimum-torque-change model for different target positions, starting from various beginning positions, is shown in Figure 8, where the predictions are plotted versus the measured torsion. For each participant we plotted the average of the measured torsion of the repeated trials for the 20 possible pairs of targets and the corresponding model predictions. Different symbols correspond to different endpoints of the movements.

As in the minimum-work model, a large part of the predictions correspond to the limit values of 0° (full elbow extension) and 180° (full elbow flexion). The other data show a significant correlation with the measured data. The correlation coefficient between measured torsion and torsion predicted according to the minimum-torque-change model was .72, which is significant on a 99% level. The slope of the linear regression fitted to the measured and predicted data in Figure

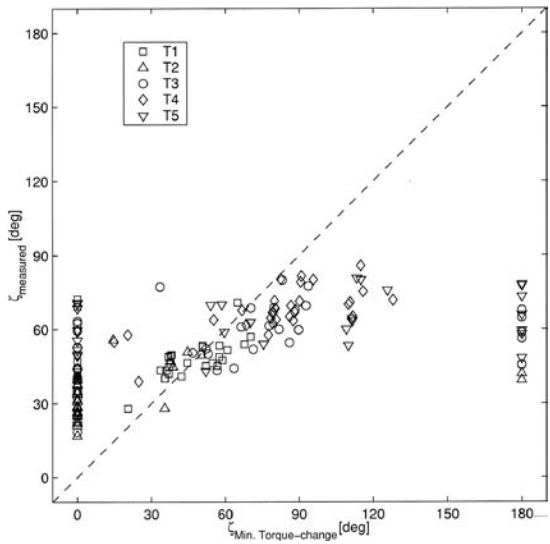

Figure 8 — Measured torsion of the upper arm vs. the predicted torsion according to the minimum-torque-change model. Data are shown for all participants. Different symbols correspond to torsion at different final targets. For each participant, the measured torsion is averaged over all movements between a pair of targets. The predicted amount of torsion is calculated based on the average initial postures of trials with the same initial and end targets.

8 was .3, however, close to the slope of the linear regression through the data for minimization of work in Figure 7 but significantly different from unity.

For many target pairs, the predictions by the two minimization models are similar. Figure 9 shows the relation between the predictions of the two models. For each participant we plotted the average of the predicted torsion for all 20 pairs of initial and final targets according to the minimum-torque-change model versus the predicted torsion according to the minimum-work model. Different symbols correspond to data from different participants.

Figure 9 shows that for some target pairs, the minimum torque change reaches a limit of 0° or 180°, whereas the minimum-work model does not. For the target pairs that did not result in a prediction near the extremes, the two models often agree ($R = .78$, $p < .01$), and the slope of a linear regression through the relevant data in Figure 9 is .73.

Discussion

This study concentrated on whether the kinematics of arm postures can be described by one of the various models for human motor control that have been proposed in the literature. Many different types of models have been proposed, but, as far as we know, no study has compared the performance of various models with experimental data on movements in 3-D. We compared the predictions by Donders's law and by

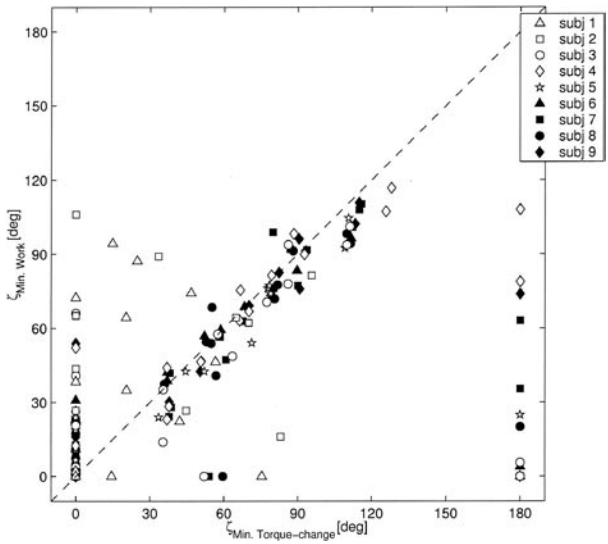

Figure 9 — Predicted torsion of the upper arm according to the minimum-torque-change model vs. the predicted torsion according to the minimum-work model. Different symbols refer to data from different participants. For each participant, the measured torsion is averaged over all repeated trials between a pair of targets, such that each target pair is presented once for each participant.

the minimum-work and minimum-torque-change models with experimental data for a well-defined set of goal-directed movements. The first conclusion is that none of the models could give a good prediction for the data. The experimental data revealed significant and systematic deviations from the predicted postures.

For pointing movements with the extended arm along a closed trajectory, arm torsion increased after the first cycles. This accumulation appears similar to results of Klein Breteler et al. (2003), who studied reaching movements that included elbow flexion through consecutive triple segments (triangles) to assess the validity of Donders's law for repetitive drawing movements. The authors reported that in most cases, the elevation of the elbow at the end of the first segment of the triangle increased after each cycle. The amount of increase of elbow elevation depended on the relative positions of the three targets that defined the corners of the triangles. The increase in torsion violates Donders's law, which requires that torsion for each pointing direction be the same, irrespective of any previous movements. A change in torsion for these cyclic movements corresponds to the predictions of the minimum-work (Soechting et al., 1995) and minimum-torque-change model (Uno et al., 1989). The observed increase in torsion (typically 5–15°), however, which is quantitatively in agreement with variations in torsion for movements along a triangle (see Klein Breteler et al., 2003), was much smaller than that predicted by these models (about 49° per cycle) and was expected to be in opposite directions for clockwise versus counterclockwise cycles. The data revealed that changes in torsion were in the same direction for clockwise- versus counterclockwise-movement cycles. Moreover, the minimization models predict that torsion increases or decreases by the same amount after each cycle, resulting in an accumulation of torsion. At first glance, Figure 4 might suggest that torsion saturates after a few movement cycles. Any saturation, however, is unlikely to be the result of reaching the extremes of the physiological range of movement. The range of torsion of the upper arm in the shoulder is about 180°, although the range of torsion in Figure 4 is about 15°. If the data in Figure 4 suggest any saturation, it must reflect a consequence of neural control rather than of biomechanics or of musculoskeletal anatomy.

One alternative model is the minimum-variance model (Harris & Wolpert, 1998). Although we did not explicitly simulate this model, it is easy to explain that the its predictions for pointing movements with the extended arm are identical to the predictions by the minimum-work and minimum-torque-change models. The minimum-variance model assumes that noise increases with force. Therefore, minimization of endpoint variability corresponds to minimization of exerted force during the movement. Minimization of exerted force requires that movements with the extended arm be made by a single-axis rotation along the shortest path, just as predicted by the minimum-work and minimum-torque-change models. Therefore, our data are not compatible with the predictions by the minimum-variance model of Harris and Wolpert (1998). The same holds for the minimum-commanded-torque-change model of Nakano et al. (1999) and the movement strategy proposed in the knowledge model (Rosenbaum et al., 1995), which corresponds to minimization of angular jerk between given initial and end postures.

Our data demonstrate that neither a posture-based model (such as Donders's law) nor a trajectory-based model can explain the experimental data. The

experimental data fall between the predictions by these two types of models. This is in agreement with results of Vetter et al. (2002), who concluded that movement strategies reflect a combination of posture-based and trajectory-based constraints. Our results and those of Vetter et al. are, at least qualitatively, in agreement with those of previous studies on adaptation to kinematic and dynamic transformations (see, e.g., Flanagan et al., 1999; Krakauer et al., 2000; Tong et al., 2002), which have shown that adaptation to changes in kinematic and dynamic transformations is achieved separately. Performance in a task where both transformations are present is better after separate adaptation to changes in kinematic and dynamic transformations than without previous adaptation. The adaptation for each of the two components (kinematic and dynamic) in the task where both transformations are present is, however, less than the adaptation achieved for the separate transformations (see Flanagan et al., 1999). This indicates that kinematic and dynamic transformations are not learned completely independently, suggesting that a strict distinction between posture-based models and trajectory-based models is an oversimplification.

Varying the constraints under which the participants had to perform the cyclic movements (fast or accurate) had some effect on the performance of the movements (see Figure 4). This is compatible with earlier experimental data of Tweed and Vilis (1992), who found that normal movements of the head obey Donders's law but that instructions to the participant to move as fast as possible between two fixation directions leads to violations of Donders's law, compatible with a minimum-energy strategy. These results suggest that normal movements might be the result of various constraints on human movement generation and that variations in instruction to participants lead to differences in the ways in which various constraints affect the movement.

For the reaching movements to targets within reaching space we found similar results. Torsion for postures to reach a particular position in space did depend on the trajectory toward the target, in a manner similar to that reported by Soechting et al. (1995) and Gielen et al. (1997). Obviously, this violates Donders's law. The variations in torsion of the upper arm as a function of initial position before the movement were qualitatively in agreement with the predictions by the minimum-work hypothesis. Quantitatively, however, they substantially disagreed.

In a previous study, Okadome and Honda (1999) compared the trajectory of sequential movements with predictions by various models. They reported that experimental movement trajectories were not compatible with the predictions by the minimum-jerk model, the equilibrium hypothesis, and the minimum-torque-change model. They concluded that the data could be explained by a model that is a weighted combination of the minimum-jerk-trajectory and the segmented minimum-angular-jerk model. These authors, however, only considered movements in a horizontal plane. For movements in a 2-D horizontal plane the complex issues related to rotations in joints with three degrees of freedom are not relevant, and expanding the workspace to 3-D space might lead to a different weighting and maybe to other constraints and more optimization parameters.

One could speculate whether some of the assumptions underlying the models evaluated in the present study in 3-D space might be responsible for the large differences between the experimental data and the predictions by the

models. One concern is the neglect of the effect of gravity in the minimum-work and the minimum-torque-change models. In our view, there is good evidence that incorporating gravity will not improve the predictions by the models, because a study by Nishikawa et al. (1999) showed that final postures do not depend on the velocity with which a movement is performed. This speed invariance of arm postures indicates that final posture only depends on dynamic forces, such as those related to acceleration of the arm and Coriolis forces, and does not depend on static force components such as antigravity force components that act during the whole movement time. Nishikawa et al. (1999) conclude that gravity does not affect final posture, suggesting that the neglect of gravity in the models has no effect on the disagreement between the predicted and measured data.

Another issue concerns the dependence of arm postures on the previously adopted postures. Several studies (Gielen et al., 1997; Soechting et al., 1995) have shown that arm postures depend on previous postures, thus raising the question whether postures also depend on the next-to-last posture. Soechting et al. (1995) showed that variability in posture is smallest for targets at the lower left. Therefore, in our study each pair of initial and end targets was preceded by the lower left target (Target 4), to minimize the variability in the initial posture. A typical sequence, therefore, would be Target 4–Target 1–Target 3, where only the posture at the end of the movement from Target 1 to Target 3 was evaluated. Although Figure 5D illustrates that the variability at Target 4 is not completely absent, it is only a few degrees, and it is highly unlikely to have a large effect on the following posture ("initial posture") or on the next posture ("end posture").

The careful reader will have noticed a difference between the data in our Figure 7 and those in Figure 8 by Soechting et al. (1995)■. The slope of the data in Figure 7 that shows measured torsion against torsion predicted by the minimum-work model is much lower than 1 (about .3), whereas the similar figure in Soechting et al. shows data that lie more or less along the line of unity. As explained earlier in the Methods section and more extensively in the Appendix, the model described by Soechting et al. contained errors. To test whether these errors might explain the difference, we have simulated the model by Soechting and colleagues, using their incorrect equations. This model leads to a better correspondence to the data by Soechting et al. in that the slope of the regression line increased to .5. This suggests that the apparently good fit between measured and simulated data in Figure 8 of Soechting et al. might be partly the result of the omission of terms in the equations used to simulate the minimum-work model in their article.

Further Considerations

Recently, several variations have been presented as alternatives to the minimum-torque-change model, such as the minimum-variance theory (Harris & Wolpert, 1998), the minimum-muscle-tension model (Dornay et al., 1996) and the minimum-commanded-torque-change model (Nakano et al., 1999). The minimum-variance theory provides a simple, unifying, and powerful principle that can be applied to goal-directed movements. It suggests that signal-dependent noise plays a fundamental role in motor planning (Harris & Wolpert, 1998). The minimum-

variance theory predicts, as do the minimum-work and minimum-torque-change models, the shortest-path strategy for the pointing movements. As explained earlier, movements along the shortest path are incompatible with the measured data. Therefore, the minimum-variance model cannot predict the results of the pointing experiments.

From a biological point of view, the minimum-muscle-tension model (Dornay et al., 1996) might seem more plausible than the others. Because the central nervous system controls only the muscles to orient a joint, a model stating that movements are optimized in muscle space might seem more plausible than one stating that movements are optimized in joint space. Simulating arm movements with a minimum-muscle-tension-change model, however, requires many more model parameters, such as optimum muscle length and muscle-attachment sites, which introduces many more degrees of freedom and induces many free parameters. Modeling all these degrees of freedom and dealing with the variability in anatomy between participants caused too much variability in the simulations to allow an accurate quantitative comparison with experimental data.

The minimum-commanded-torque-change model presented by Nakano and colleagues (1999) is rather similar to the minimum-torque-change model, the only differences being the values of the parameters for inertia and viscosity. Thus, the predictions with the minimum-command-torque-change model will be compatible with the predictions by the minimization models tested in the present study and that appeared to produce predictions that did not agree with experimental observations.

In summary, our results demonstrate that there is no single model that can accurately predict the experimental data. The results suggest that motor control is based on a combination of control principles, optimizing a task-dependent combination of constraints, in line with the theory suggested by Todorov and Jordan (2002).

References

Donders, F.C. (1848). Beitrag zur lehre von den Bewegungen des menschlichen Auges. *Holländische Beiträge zu den anatomischen und physiologischen Wissenschaften*, **1**, 104-145.

Dornay, M., Uno, Y., Kawato, M., & Suzuki, R. (1996). Minimum muscle-tension change trajectories predicted by using a 17-muscle model of the monkey's arm. *Journal of Motor Behavior*, **28**, 83-100.

Flanagan, J.R., Nakano, E., Imamuzi, H., Osu, R., Yoshioka, T., & Kawato M. (1999). Composition and decomposition of internal models in motor learning under altered kinematic and dynamic environments. *Journal of Neuroscience*, **19**, RC34.

Flash, T. (1987). The control of hand equilibrium trajectories in multi-joint arm movements. *Biological Cybernetics*, **57**, 257-274.

Georgopoulos, A.P., Kalaska, J.F., & Massey, J.T. (1981). Spatial trajectories and reaction times of aimed movements: Effects of practice, uncertainty and change in target location. *Journal of Neurophysiology,* **46**, 725-743.

Gielen, C.C.A.M., Vrijenhoek, E.J., Flash, T., & Neggers, S.F.W. (1997). Arm position constraints during pointing and reaching in 3-D space. *Journal of Neurophysiology,* **78**, 660-673.

Gielen, S.C. (1993). Movement dynamics. *Current Opinion in Neurobiology,* **3**, 912-916.

Harris, C.M., & Wolpert, D.M. (1998). Signal-dependent noise determines motor planning. *Nature,* **394**, 780-784.

Haruno, M., Wolpert, D.M., & Kawato, M. (1999). Multiple paired forward-inverse models for human motor learning and control. *Advances in Neural Information Processing Systems*, **11**, 31-37.

Haruno, M., Wolpert, D.M., & Kawato, M. (2001). Mosaic model for sensorimotor learning and control. *Neural Computation,* **13**, 2201-2220.

Haustein, W. (1989). Considerations on Listing's law and the primary position by means of a matrix description of eye position control. *Biological Cybernetics,* **60**, 411-420.

Hogan, N. (1985). The mechanics of multi-joint posture and movement. *Biological Cybernetics*, **52**, 315-331.

Hore, J., Watts, S., & Vilis, T. (1992). Constraints on arm position when pointing in three dimensions: Donders' law and the Fick gimbal strategy. *Journal of Neurophysiology*, **68**, 374-383.

Klein Breteler, M.D., Hondzinski, J.M., & Flanders, M. (2003). Drawing sequences of segments in 3D: Kinetic influences on arm configuration. *Journal of Neurophysiology*, **89**, 3253-3263.

Krakauer, J.W., Pine, Z.M., Ghilardi, M-F., & Ghez, C. (2000). Learning of visuomotor transformations for vectorial planning of reaching trajectories. *Journal of Neuroscience*, **20**, 8916-8924.

Medendorp, W.P., Crawford, J.D., Henriques, D.Y.P., Van Gisbergen, J.A.M., & Gielen, C.C.A.M. (2000). Kinematic strategies for upper-arm forearm coordination in three dimensions. *Journal of Neurophysiology*, **84**, 2302-2316.

Miller, L.E., Theeuwen, M., & Gielen, C.C.A.M. (1992). The control of arm pointing movements in three dimensions. *Experimental Brain Research*, **90**, 415-426.

Nakano, E., Imamizu, H., Osu, R., Uno, Y., Gomi, H., Yoshioka, T., & Kawato, M. (1999). Quantitative examinations of internal representations for arm trajectory planning: Minimum commanded torque change model. *Journal of Neurophysiology*, **81**, 2140-2155.

Nishikawa, K.C., Murray, S.T., & Flanders, M. (1999). Do arm postures vary with the speed of reaching? *Journal of Neurophysiology*, **81**, 2582-2586.

Okadome, T., & Honda, M. (1999). Kinematic construction of the trajectory of sequential arm movements. *Biological Cybernetics*, **80**, 157-169.

Rosenbaum, D.A., Loukopoulos, L.D., Meulenbroek, R.G.J., Vaughan, J., & Engelbrecht, S.E. (1995). Planning reaches by evaluating stored postures. *Psychological Review*, **102**, 28-67.

Soechting, J.F., Buneo, C.A., Herrmann, U., & Flanders, M. (1995). Moving effortlessly in three dimensions: Does Donders' law apply to arm movement? *Journal of Neuroscience*, **15**, 6271-6280.

Soechting, J.F., & Lacquaniti, F. (1981). Invariant characteristics of a pointing movement in man. *Journal of Neuroscience*, **1**, 710-720.

Stoker, J.J. (1969). *Pure and applied mathematics: Vol. XX. Differential geometry*. New York: Wiley Interscience.

Straumann, D., Haslwanter, T., Hepp-Reymond, M.C., & Hepp, K. (1991). Listing's law for eye, head and arm movements and their synergistic control. *Experimental Brain Research*, **86**, 209-215.

Todorov, E., & Jordan, M.I. (2002). Optimal feedback control as a theory of motor coordination. *Nature Neuroscience*, **5**, 1226-1235.

Tong, C., Wolpert, D.M., Flanagan, J.R. (2002). Kinematic and dynamics are represented independently in motor working memory: Evidence from an interference study. *Journal of Neuroscience*, **22**, 1108-1113.

Tweed, D., & Vilis, T. (1987). Implications of rotational kinematics for the oculomotor system in three dimensions. *Journal of Neurophysiology*, **58**, 832-849.

Tweed, D., & Vilis, T. (1992). Listing's law for gaze directing head movements. In A. Berthoz, P.P. Vidal, & W. Graf (Eds.), *The head-neck sensory-motor system* (pp. 387-391). New York: Oxford University Press.

Uno, Y., Kawato, M., & Suzuki, R. (1989). Formation and control of optimal trajectory in human multi-joint arm movement. Minimum torque-change model. *Biological Cybernetics*, **61**, 89-101.

Vetter, P., Flash, T., & Wolpert, D.M. (2002). Planning movements in a simple redundant task. *Current Biology*, **12**, 488-491.

Appendix

This appendix provides a full derivation of the equations that underlie the minimum-work model. Although it is rather straightforward, we provide the detailed derivation because the results differ from the equations in Soechting et al. (1995), where a few terms are missing.

The angle η refers to rotations about the vertical Z axis and determines the yaw angle of the arm. A rotation η determines the arm's azimuth. The second angle, θ, determines the arm's elevation, and the third angle, ς, refers to rotations about the humeral axis of the upper arm. This rotation does not change the location of the elbow but does affect the location of the hand in space when the elbow is flexed. We also define ϕ as the angle of elbow flexion; $\phi = 0$ corresponds to full extension.

With these definitions, the location of the elbow $[X_e, Y_e, Z_e]$ is given by

$$\begin{aligned} X_e &= -L_u \sin\eta \sin\theta \\ Y_e &= -L_u \cos\eta \sin\theta \\ Z_e &= -L_u \cos\theta \end{aligned} \tag{Ia}$$

where L_u represents the length of the upper arm.

The location of the index finger $[X_f, Y_f, Z_f]$ is given by

$$\begin{aligned} X_f &= X_e - L_f[\sin\varphi(\cos\varsigma \sin\eta \cos\theta + \sin\varsigma \cos\eta) + \cos\varphi(\sin\eta \sin\theta)] \\ Y_f &= Y_e + L_f[\sin\varphi(\cos\varsigma \cos\eta \cos\theta - \sin\varsigma \sin\eta) + \cos\varphi(\cos\eta \sin\theta)] \\ Z_f &= Z_e + L_f[\sin\varphi(\cos\varsigma \sin\theta) - \cos\varphi(\cos\theta)] \end{aligned} \tag{Ib}$$

where L_f refers to the length of the forearm.

The amount of work, W, necessary to move the arm from one point to another is given by Eq. 2. With the definitions of the coordinate system related to the upper

arm, we can derive Eq. 3 in the main text by using the velocity v_u for the center of mass of the upper arm,

$$v_u = \begin{bmatrix} -\frac{1}{2} L_u \Omega_Y \\ -\frac{1}{2} L_u \Omega_X \\ 0 \end{bmatrix} \tag{II}$$

and v_f for the center of mass of the forearm:

$$v_f = \begin{bmatrix} -\Omega_Y \left(L_u + \frac{L_f}{2} \cos\phi \right) - \Omega_Z \left(\frac{L_f}{2} \sin\phi \right) \\ \Omega_X \left(L_u + \frac{L_f}{2} \cos\phi \right) + \dot{\phi} \left(\frac{L_f}{2} \cos\phi \right) \\ \Omega_X \left(\frac{L_f}{2} \sin\phi \right) + \dot{\phi} \left(\frac{L_f}{2} \sin\phi \right) \end{bmatrix} \tag{III}$$

With these definitions, the first part of the equation for the total amount of work corresponds to

$$\begin{aligned} \frac{1}{2} m \bar{v}^T \cdot \bar{v} &= \frac{m_u}{2} \bar{v}_u^T \cdot \bar{v}_u + \frac{m_f}{2} \bar{v}_f^T \cdot \bar{v}_f \\ &= \frac{m_u}{2} \left[\frac{L_u}{4} \Omega_Y^2 + \frac{L_u}{4} \Omega_X^2 \right] \\ &+ \frac{m_f}{2} \left[\Omega_Y^2 \left(L_u + \frac{L_f}{2} \cos\phi \right)^2 + 2\Omega_Y \Omega_Z \left(L_u + \frac{L_f}{2} \cos\phi \right) \left(\frac{L_f}{2} \sin\phi \right) + \Omega_Z^2 \frac{L_f^2}{4} \sin\phi \right. \\ &\quad + \Omega_x^2 \left(L_u + \frac{L_f}{2} \cos\phi \right)^2 + 2\Omega_X \dot{\phi} \left(L_u + \frac{L_f}{2} \cos\phi \right) \left(\frac{L_f}{2} \cos\phi \right) + \dot{\phi}^2 \frac{L_f^2}{4} \cos\phi \\ &\quad \left. + \Omega_x^2 \frac{L_f^2}{4} \sin^2\phi + 2\Omega_X \dot{\phi} \frac{L_f^2}{4} \sin^2\phi + \dot{\phi}^2 \frac{L_f^2}{4} \sin^2\phi \right] \end{aligned} \tag{IV}$$

The rotational part of the total work corresponds to the sum of a part for rotations of the upper arm,

$$\frac{1}{2} \Omega^T I \Omega = \frac{1}{2} \begin{pmatrix} \Omega_X \\ \Omega_Y \\ \Omega_Z \end{pmatrix} \cdot \begin{pmatrix} I_{u1} \\ I_{u1} \\ I_{u2} \end{pmatrix} \cdot \begin{pmatrix} \Omega_X \\ \Omega_Y \\ \Omega_Z \end{pmatrix} \tag{V}$$

and a part for rotations of the forearm:

$$\frac{1}{2} \Omega^T I \Omega = \frac{1}{2} \begin{pmatrix} \Omega_X + \dot{\phi} \\ \Omega_Y \cos\phi + \Omega_Z \sin\phi \\ \Omega_Y \sin\phi - \Omega_Z \cos\phi \end{pmatrix} \cdot \begin{pmatrix} I_{u1} \\ I_{u1} \\ I_{u2} \end{pmatrix} \cdot \begin{pmatrix} \Omega_X + \dot{\phi} \\ \Omega_Y \cos\phi + \Omega_Z \sin\phi \\ \Omega_Y \sin\phi - \Omega_Z \cos\phi \end{pmatrix} \tag{VI}$$

With the preceding equations and the following abbreviations

$$
\begin{aligned}
I_1 &= I_{u1} + m_u \frac{L_u^2}{4} + m_f L_u^2 \\
I_2 &= U_{u2} \\
I_3 &= m_f \frac{L_f^2}{4} + I_{f1} \\
I_4 &= I_{f2} \\
A &= m_f L_u \frac{L_f}{2}
\end{aligned}
\qquad \text{(VII)}
$$

the total work is derived to correspond to

$$
\begin{aligned}
W = \frac{1}{2}\Big[& I_1\left(\Omega_X^2 + \Omega_Y^2\right) + I_2\Omega_Z^2 \\
& + I_3\left(\left(\Omega_x + \dot{\phi}\right)^2 + \left(\Omega_Y \cos\phi + \Omega_Z \sin\phi\right)^2\right) + I_4\left(\Omega_Y \sin\phi - \Omega_Z \cos\phi\right)^2 \\
& + 2A\left(\left(\Omega_X^2 + \Omega_Y^2\right)\cos\phi + \Omega_Z\Omega_Y \sin\phi + \dot{\phi}\Omega_X \cos\phi\right)\Big]
\end{aligned}
\qquad \text{(VIII)}
$$

Two terms in this equation differ from the equation for the total amount of work presented by Soechting et al. (1995). Because we started with the same equations for the angular velocities as Soechting and colleagues, we expect the difference in equations to be the result of printing errors in Soechting's equation. The difference includes three extra terms in the total work corresponding to

$$
\text{extra} = \frac{A}{2}\left[\left(\Omega_X^2 + \Omega_Y^2\right)\cos\phi + \Omega_Z\Omega_Y \sin\phi + 2\dot{\phi}\Omega_X \cos\phi\right] \qquad \text{(IX)}
$$

The total work done during the movement from the starting location to the target is zero. The positive work done to accelerate the arm initially is canceled by the negative work required to decelerate the arm at the end of the movement. The work will assume a peak positive value when the torque changes sign from positive to negative, that is, at the peak of the velocity. The posture of the arm at the end of the movement is such that the peak work, *W*, is minimized, provided that the arm reaches the target.